

# The Evidence Theory Based Post-Processing of Colour Images

Marija BACAUSKIENE

*Department of Applied Electronics, Kaunas University of Technology  
LT-3031, Kaunas, Lithuania  
e-mail: marija.bacauskiene@ktu.lt*

Antanas VERIKAS

*Department of Applied Electronics, Kaunas University of Technology &  
Intelligent Systems Laboratory, Halmstad University  
Box 823, S 301 18 Halmstad, Sweden  
e-mail: antanas.verikas@ide.hh.se*

Received: January 2004

**Abstract.** The problem of post-processing of a classified image is addressed from the point of view of the Dempster–Shafer theory of evidence. Each neighbour of a pixel being analyzed is considered as an item of evidence supporting particular hypotheses regarding the class label of that pixel. The strength of support is defined as a function of the degree of uncertainty in class label of the neighbour, and the distance between the neighbour and the pixel being considered. A post-processing window defines the neighbours. Basic belief masses are obtained for each of the neighbours and aggregated according to the rule of orthogonal sum. The final label of the pixel is chosen according to the maximum of the belief function.

**Key words:** evidence theory, colour image segmentation, classification, post-processing.

## 1. Introduction

Colour image processing and analysis is increasingly used in industry, medical applications and other fields. Quality inspection, process control, material analysis, medical image processing are a few examples (Onyango and Marchant, 2001; Verikas *et al.*, 2000; Xu *et al.*, 1999). It is obvious that the use of colour image processing in various fields of human activity will considerably grow in the near future. Therefore, development of efficient computational models for real world problems is of crucial importance. Image segmentation is one of the most widely used procedures in various applications of image processing technologies.

Various colour image segmentation techniques have been proposed. The most commonly used approaches include: histogram thresholding (Kuru *et al.*, 2001), feature /colour space clustering (Li and Yuen, 2000; Tominaga, 1992), edge detection approaches (Xu *et al.*, 1999; Trahanias and Venetsanopoulos, 1996), neural network based

approaches (Huang *et al.*, 2002; Papamarkos *et al.*, 2000; Verikas *et al.*, 1994; Verikas *et al.*, 1993), region-based approaches (Cheng *et al.*, 2002; Tremeau and Borel, 1997), Markov random fields (Gao *et al.*, 2002) and mixture-of-Gaussians modelling (Greenspan *et al.*, 2001), physics based approaches (Onyango and Marchant, 2001), and combinations of above (Chen and Lu, 2002; Mirmehdi and Petrou, 2000). A recent survey of colour image segmentation methods can be found in (Cheng *et al.*, 2001).

All the existing colour image segmentation approaches are strongly application dependent and suffer from different characteristic drawbacks. For example, histogram thresholding does not consider spatial details and does not work well for images without obvious peaks and valleys. Feature space clustering based methods do not utilize spatial information too. How to select features for obtaining satisfactory segmentation results remains unclear. Region-based approaches are quite expensive in computation time and sensitive to the examination order of regions and pixels. Edge detection approaches are quite sensitive to noise and do not work well for images containing ill-defined edges. Neural network based approaches usually require long training time and initialization may affect the results. Markov random fields modelling is quite expensive in computation time.

A segmented image can be viewed as an image of class labels – a pixel-wise classified image, – where a class label is available for each pixel of the image. To improve segmentation results various image post-processing procedures are often applied. Post-processing is a common technique for improving recognition accuracy of strings or images (Bouchaffra *et al.*, 1999; Chen *et al.*, 1994; Verikas and Malmqvist, 1995; Song *et al.*, 1995; Verikas *et al.*, 1994). Amongst others, the non-stationary Markov models (Bouchaffra *et al.*, 1999) and the probabilistic relaxation labelling (Song *et al.*, 1995) are two most often used approaches to tackle the problem. Both of the approaches are rather time consuming. For example, the basic idea of the probabilistic relaxation labelling algorithm is to make use of contextual information conveyed by the neighbouring pixels to update iteratively the label probability distribution in each pixel location until convergence to a consistent assignment of labels is achieved. In this paper, the problem of post-processing of a segmented image is addressed from the point of view of the Dempster–Shafer theory of evidence.

The Dempster–Shafer theory of evidence (Shafer, 1976) has been used by several authors in different applications as a tool for representing and combining items of evidences. Applications can be found in fusion of outputs of several classifiers (Xu *et al.*, 1992), analysis of medical images (Bloch, 1996; Chen *et al.*, 1993), generalization of the  $k - NN$  classifier (Denoeux, 1995), object detection (van Cleynenbreugel *et al.*, 1991), and remote sensing classification (LeHegarat-Masclé *et al.*, 1997; Pinz *et al.*, 1996). We use the evidence theory to post-process pixel-wise classified colour images. We assume that for each pixel of an image analyzed, information is available about the degree of doubt in the class label of the pixel. We consider each neighbour of a pixel being analyzed as an item of evidence supporting particular hypotheses regarding the class label of that pixel. A post-processing window defines the neighbours. The items of evidence are then combined to obtain the final class label estimate of the pixel being considered.

The remainder of the paper is organized as follows. In the next section we briefly describe the colour space used. Section 3 presents the background information on the evidence theory. The image post-processing approach proposed is described in Section 4. Section 5 presents the results of the experimental investigations. Finally, Section 6 presents conclusions of the work.

## 2. Colour Space Used

Colour image acquisition equipment such as a *CCD* colour camera obtains the *RGB* values, which can be directly used for representing colours in the *RGB* colour space. However, different acquisition equipment gives us different *RGB* values for the same incident light. One more drawback of the *RGB* colour space is that the metrics does not represent colour differences in a uniform scale, making it difficult to evaluate the similarity of two colours from their distance in the space.

To meet the requirement of uniformity of distribution of colours the Commission Internationale de l'Eclairage (CIE) has recommended using one of two alternative colour spaces:  $L^*u^*v^*$  or  $L^*a^*b^*$  colour space (Hunt, 1991; Wyszecki and Stiles, 1982). It is common practice to use the  $L^*a^*b^*$  colour space for describing absorbing materials such as pigments and dyes (Verikas *et al.*, 2000). We used the  $L^*a^*b^*$  colour space in this work.

To map the *RGB* values into the  $L^*a^*b^*$  colour space, the *RGB* values are first transformed to the *XYZ* tristimulus values as follows:

$$X = a_{11}R + a_{12}G + a_{13}B, \quad (1)$$

$$Y = a_{21}R + a_{22}G + a_{23}B, \quad (2)$$

$$Z = a_{31}R + a_{32}G + a_{33}B \quad (3)$$

with the coefficients  $a_{ij}$  being determined by a colourimetric characterization of the hardware used. Having *XYZ* tristimulus values the  $L^*a^*b^*$  colour space is defined as (Wyszecki and Stiles, 1982):

$$L = 116(Y/Y_n)^{1/3} - 16, \quad \text{if } Y/Y_n > 0.008856, \quad (4)$$

$$L = 903.3(Y/Y_n), \quad \text{if } Y/Y_n \leq 0.008856, \quad (5)$$

$$a^* = 500[(X/X_n)^{1/3} - (Y/Y_n)^{1/3}], \quad (6)$$

$$b^* = 200[(Y/Y_n)^{1/3} - (Z/Z_n)^{1/3}], \quad (7)$$

where  $X_n, Y_n, Z_n$  are the tristimulus of *X, Y, and Z* for the appropriately chosen reference white. If any of the ratios  $X/X_n, Y/Y_n,$  and  $Z/Z_n$  is equal to or less than 0.008856, it is replaced in the above formulae by:

$$7.7877f + 16/116, \quad (8)$$

where  $f$  is  $X/X_n$ ,  $Y/Y_n$ , or  $Z/Z_n$ , as the case may be (Wyszecki and Stiles, 1982). The Euclidean distance measure can be used to measure the distance ( $\Delta E$ ) between the two points representing the colours in the colour space:

$$\Delta E = [(\Delta L^*)^2 + (\Delta a^*)^2 + (\Delta b^*)^2]^{1/2}. \quad (9)$$

### 3. The Theory of Evidence

Let  $\Theta$  be a finite set of mutually exclusive and exhaustive atomic hypotheses about some problem domain. The set  $\Theta = \{\theta_1, \theta_2, \dots, \theta_M\}$  is called the *frame of discernment* (Bloch, 1996). Let  $2^\Theta$  denote the power set of  $\Theta$ . A function  $m: 2^\Theta \rightarrow [0, 1]$  is called a basic probability assignment if

$$m(\emptyset) = 0, \quad (10)$$

$$\sum_{A \subseteq \Theta} m(A) = 1. \quad (11)$$

The probability theory assigns *probabilities* to atomic hypotheses  $\theta_i$ , while a *basic probability number*  $m(A)$  represents one's *belief* in a not necessarily atomic hypothesis  $A$ . For a compound hypothesis  $A \neq \theta_i$ ,  $m(A)$  measures our belief that we are willing to commit to  $A$ . The belief cannot be subdivided amongst the subsets of  $A$  and is assigned to  $A$  at the expense of support  $m(\theta_i)$ . The fact of having  $m(\Theta) = 1$  characterizes the total ignorance. The belief in  $A$  and the belief in its negation  $\bar{A}$  do not necessarily sum to 1.

A support committed to a compound hypothesis  $A$  should also be committed to the hypotheses it implies. Therefore, to obtain the total belief in  $A$ , we must add to  $m(A)$  the basic probability numbers  $m(B)$  for all subsets  $B$  of  $A$ . If  $m$  is a basic probability assignment, then a function  $Bel: 2^\Theta \rightarrow [0, 1]$

$$Bel(A) = \sum_{B \subseteq A} m(B). \quad (12)$$

The subsets  $B$  of  $\Theta$  for which  $m(B) > 0$  are called the *focal elements* of the belief function. The union of the focal elements is called the *core* of the belief function. The belief functions having only one focal element in addition to  $\Theta$  are called *simple support functions*.  $Bel$  is a simple support function if there exists a focal element  $F \subseteq \Theta$ ,  $Bel(\Theta) = 1$  and

$$Bel(A) = \begin{cases} s, & \text{if } F \subseteq A \text{ and } A \neq \Theta, \\ 0, & \text{otherwise,} \end{cases} \quad (13)$$

where  $s$  is called *degree of support* of  $Bel$ . We use simple support functions in our application.

Given two basic probability assignments  $m_1$  and  $m_2$  associated with  $Bel_1$  and  $Bel_2$  induced by two different sources of information over the same frame of discernment  $\Theta$  can be combined into a single belief function if their cores are not disjoint. The Dempster's rule of combination or *orthogonal sum* is a convenient way for performing such a combination. The orthogonal sum  $m = m_1 \oplus m_2, m: 2^\Theta \rightarrow [0, 1]$  is defined as:

$$m(\emptyset) = 0, \tag{14}$$

$$m(A) = K^{-1} \sum_{B \cap D = A} m_1(B)m_2(D), \quad A \neq \emptyset, \tag{15}$$

where

$$K = \sum_{B \cap D \neq \emptyset} m_1(B)m_2(D). \tag{16}$$

The function  $m$  is a basic probability assignment. The core of  $Bel$  given by  $m$  equals the intersection of the cores of  $Bel_1$  and  $Bel_2$ . The combination rule is commutative and associative, and it may be generalized to combine multiple evidences.

Let  $F$  be a focal element for two simple support functions  $Bel_1$  and  $Bel_2$  with degrees of support  $s_1$  and  $s_2$ , respectively. If  $Bel = Bel_1 \oplus Bel_2$  and  $m$  is associated with  $Bel$  then

$$m(F) = 1 - (1 - s_1)(1 - s_2), \tag{17}$$

$$m(\Theta) = (1 - s_1)(1 - s_2), \tag{18}$$

$$m(A) = 0, \quad \forall A \in 2^\Theta \setminus \{F, \Theta\}. \tag{19}$$

#### 4. The Approach

Suppose we are given a pixel-wise classified colour image. A post-processing window centered on the pixel being considered, as shown in Fig. 1, defines a set of labelled (classified) neighbours of that pixel. We consider each member of the set as an item of evidence supporting particular hypotheses regarding the class label of the pixel being considered. There are two factors the strength of the support depends on, namely the degree of doubt in the class label of the member and the distance between the member and the pixel being

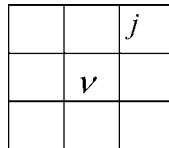


Fig. 1. A post-processing window around the pixel of interest  $\nu$ .

analyzed. We obtain the basic belief masses for each of the members of the set and aggregate them according to the rule of orthogonal sum. The final label of the pixel is chosen according to the maximum of the basic probability numbers of the atomic hypotheses.

#### 4.1. Defining the Basic Probability Assignment

Let  $\Theta = \{\theta_1, \theta_2, \dots, \theta_M\}$  be a set of  $M$  decision classes – the frame of discernment of the application. The number of the classes  $M$  is known in advance. In our case, each class is specified by a set of reference patterns obtained from clustering and learning vector quantization processes (Verikas *et al.*, 2003).

Assume that  $\mathbf{x}$  is a pixel of interest and  $X = \{\mathbf{x}^1, \mathbf{x}^2, \dots, \mathbf{x}^V\}$  is a set of  $V$  nearest neighbours of the pixel. Associated with the  $j$ th member of the set are the class label  $L^j = q$ ,  $L = \{1, 2, \dots, M\}$  and the degree of certainty  $\mu_{jq} \in [0, 1]$ , with which the label  $q$  was assigned to the  $j$ th member during the classification process based on the colour vector representing the member. We use two parameters to characterize the certainty of the classification process, namely  $\mu_{jq}^{dist}$  – the parameter, which takes into consideration the distance between the pixel  $\mathbf{x}^j$  and the closest class  $q$ , and  $\mu_{jq}^{rival}$  – the parameter depending on the difference between the distances from  $\mathbf{x}^j$  to the two closest classes. The exact definition of the parameters, based on suggestions presented in (Denoeux, 1995), will be given shortly.

Let's assume that the  $q$ th class is represented by  $N_q$  reference patterns – weight vectors. Let  $d(\mathbf{x}^j, \mathbf{w}_q^i)$  be the distance – measured according to (9) – between the input pixel  $\mathbf{x}^j$  and the  $i$ th weight vector of the  $q$ th class. Suppose that  $\mathbf{w}_q^k$  is the closest weight vector to the pixel  $\mathbf{x}^j$  amongst all the weight vectors representing the  $q$ th class:

$$k = \arg \min_{i=1,2,\dots,N_q} d(\mathbf{x}^j, \mathbf{w}_q^i), \quad q = 1, 2, \dots, M. \quad (20)$$

We assume that the distance between pixel  $\mathbf{x}^j$  and the class  $\theta_q$  is given by  $d(\mathbf{x}^j, \mathbf{w}_q^k)$  – the distance between the pixel  $\mathbf{x}^j$  and the closest weight vector  $\mathbf{w}_q^k$  representing the class  $\theta_q$ . Suppose that  $q$  and  $p$  are the indices of the closest and the next closest class, respectively, to the pixel  $\mathbf{x}^j$ . The parameters  $\mu_{jq}^{dist}$  and  $\mu_{jq}^{rival}$  we then define as:

$$\mu_{jq}^{dist} = \beta_0^{dist} \exp \left\{ -\alpha_q^{dist} d(\mathbf{x}^j, \mathbf{w}_q^k) \right\}, \quad (21)$$

$$\mu_{jq}^{rival} = 1 - \beta_0^{rival} \exp \left\{ -\alpha_q^{rival} [d(\mathbf{x}^j, \mathbf{w}_p^k) - d(\mathbf{x}^j, \mathbf{w}_q^k)] \right\}, \quad (22)$$

where  $\alpha_q^{dist}$ ,  $\alpha_q^{rival}$ ,  $\beta_0^{dist}$ , and  $\beta_0^{rival}$  are parameters and the indices  $q$  and  $p$  are given by

$$q = \arg \left\{ \min_{l=1,2,\dots,M} \left[ \min_{i=1,2,\dots,N_l} d(\mathbf{x}^j, \mathbf{w}_l^i) \right] \right\}, \quad (23)$$

$$p = \arg \left\{ \min_{l=1,2,\dots,M, l \neq q} \left[ \min_{i=1,2,\dots,N_l} d(\mathbf{x}^j, \mathbf{w}_l^i) \right] \right\}, \quad (24)$$

where  $N_l$  is the number of reference patterns – weight vectors – representing the  $l$ th class. Heuristics for choosing the parameters  $\alpha_q^{dist}$ ,  $\alpha_q^{rival}$ ,  $\beta_0^{dist}$ , and  $\beta_0^{rival}$  will be discussed shortly.

For any  $\mathbf{x}^j \in X$ , including the  $\mathbf{x}^\nu$  itself, the knowledge that  $L^j = q$  can be considered as a support of the hypothesis that  $\mathbf{x}^\nu$  belongs to  $\theta_q$ . However, the belief in hypothesis that  $L^j = q$  contains some degree of uncertainty. We find it reasonable to assume that the degree of uncertainty increases with the decrease of  $\mu_{jq}^{dist}$  and  $\mu_{jq}^{rival}$  or with the increase of the topological distance  $d(\nu, j)$  between pixels  $\nu$  and  $j$ . Since we use the simple support functions for representing evidence, we distribute the evidence obtained from the knowledge between  $\theta_q$  and the frame of discernment  $\Theta$ . Let us assume that  $L^j = p$ . The following basic probability assignment  $m^{\nu j}$  is then used for representing the evidence:

$$m^{\nu j}(\theta_q) = \beta_j, \tag{25}$$

$$m^{\nu j}(\Theta) = 1 - \beta_j, \tag{26}$$

$$m^{\nu j}(A) = 0, \quad \forall A \in 2^\Theta \setminus \{\theta_q, \Theta\}, \tag{27}$$

$$\beta_j = \beta_{pq} T \left[ T \{ \mu_{jq}^{dist}, \mu_{jq}^{rival} \}, \exp \{ -\alpha_p d(\nu, j) \} \right], \tag{28}$$

where  $T$  stands for the  $T$ -norm operator,  $0 < \beta_{pq} < 1$ , and  $\alpha_p > 0$ . From (28) follows that  $0 < \beta_j < 1$ . The coefficient  $\beta_{pq}$  expresses our initial certainty that a pixel assigned to class  $q$  in the initial classification process has value for post-processing a pixel assigned to class  $p$ . The use of  $\alpha_p$  specific for each class indicates that the influence of the distance  $d(\nu, j)$  may depend on the class of a pixel being analyzed.

For each of the  $V$  neighbours of pixel  $\mathbf{x}^\nu$  from the post-processing window the basic probability assignment is defined. Next the basic probability assignments are combined using the Dempster's rule of combination.

#### 4.2. Combining Evidence

Let  $V_q^\nu$  denote the number of neighbours of  $\mathbf{x}^\nu$  belonging to the class  $\theta_q$ . Assuming that  $V_q^\nu \neq 0$  and applying (17) and (18), we then obtain the following result of the combination of the  $V_q^\nu$  basic probability assignments:

$$m_q^\nu(\theta_q) = 1 - \prod_{L^i=q} (1 - \beta_i), \tag{29}$$

$$m_q^\nu(\Theta) = \prod_{L^i=q} (1 - \beta_i). \tag{30}$$

If  $V_q^\nu = 0$ , then  $m_q^\nu(\theta_q) = 0$  and  $m_q^\nu(\Theta) = 1$ . Following (Denoeux, 1995), we obtain the following result of the combination of all the basic probability assignments in the post-processing window:

$$m^\nu(\theta_q) = \frac{1}{K} m_q^\nu(\theta_q) \prod_{i \neq q} m_i^\nu(\Theta), \quad q = 1, \dots, M, \tag{31}$$

$$m^\nu(\Theta) = \frac{1}{K} \prod_{i=1}^M m_i^\nu(\Theta), \tag{32}$$

where the normalizing factor  $K$  is given by

$$K = \sum_{q=1}^M m_q^\nu(\theta_q) \prod_{i \neq q} m_i^\nu(\Theta) + \prod_{i=1}^M m_i^\nu(\Theta). \quad (33)$$

The final decision about the class label  $q^\nu$  of the pixel  $\mathbf{x}^\nu$  is obtained from the basic probability numbers of the atomic hypotheses:

$$q^\nu = \arg \max_{i=1, \dots, M} m_i^\nu(\theta_i). \quad (34)$$

## 5. Experimental Tests

We applied the post-processing technique for analyzing colour images taken from pulp of recycled paper. Fig. 2 presents two examples of such images. The aim of the analysis is to detect specks in the images and sort out them into several categories of sizes and colours, namely *Cyan (C)*, *Magenta (M)*, *Yellow (Y)*, *Green (G)*, and *Black (B)*. Such an analysis is utilized in the paper recycling process to characterize the quality of secondary pulps regarding the amount of rest ink particles.

Since there are five colour classes of specks, during the image segmentation process each pixel of the images is assigned into one of six colour classes including the aforementioned five and the background colour class – *White (W)*. The pixel-wise classification is based on the minimum distance classifier, having the colour classes represented by several reference patterns – weight vectors. After the segmentation the post-processing approach developed is applied to improve the segmentation results.

In total,  $N = \sum_{q=1}^M N_q = 49$  reference patterns have been used to represent the six colour classes. This number is given by a  $2D$  self-organizing map (*SOM*) of  $7 \times 7 = 49$  nodes used to represent the chromaticity of pixels found in a representative set of colour images analyzed (Verikas *et al.*, 2000). There were  $N_C = 9$ ,  $N_M = 9$ ,  $N_Y = 8$ ,  $N_G = 5$ ,  $N_B = 8$ , and  $N_W = 10$  reference patterns representing the six aforementioned colour



Fig. 2. Two examples of images taken from different pulp samples.

classes. These numbers were determined by analyzing the *SOM* and the average lightness  $L^*$  of pixels mapped onto the nodes of the map (Verikas *et al.*, 2000).

### 5.1. Parameter Settings

The parameters  $\alpha_q^{dist}$ ,  $\alpha_q^{rival}$ ,  $\beta_0^{dist}$ ,  $\beta_0^{rival}$ ,  $\beta_{pq}$ , and  $\alpha_p$  have to be fixed for determining the basic probability assignments. Different heuristics have been tested to fix the parameters. For  $\beta_0^{dist}$ ,  $\beta_0^{rival}$  and  $\beta_{pq}$  a good choice was  $\beta_0^{dist} = \beta_0^{rival} = 0.95$ ,  $\beta_{pq} = 0.9$  if  $p = q$  and  $\beta_{pq} = 0.8$ , if  $p \neq q$ . The parameters affect the subdivision of our belief obtained from some knowledge between the atomic hypotheses  $\theta_i$  and the frame of discernment  $\Theta$ . The same value of the parameter  $\alpha_p$  has been used for all the colour classes considered. The parameter controls the influence of the distance  $d(\nu, j)$  on the basic probability numbers. We used the Euclidean distance measure to measure the distance. To determine the parameter  $\alpha_q^{dist}$ , we used the heuristic presented in (Denoeux, 1995). The parameters  $\alpha_q^{dist}$  and  $\alpha_q^{rival}$  were determined separately for each class,  $\alpha_q^{dist} = 1/d_q^{dist}$  and  $\alpha_q^{rival} = 1/d_q^{rival}$ , where  $d_q^{dist}$  is the average distance between two training vectors belonging to class  $\theta_q$ , and  $d_q^{rival}$  is given by the difference between the average distances  $\bar{d}(\mathbf{x}, \mathbf{w}_q^k)$  and  $\bar{d}(\mathbf{x}, \mathbf{w}_p^k)$ , where  $\bar{d}(\mathbf{x}, \mathbf{w}_q^k)$  is the average distance of vectors coming from the class  $\theta_q$  to the nearest reference vector representing the class  $\theta_q$ , and  $\bar{d}(\mathbf{x}, \mathbf{w}_p^k)$  is the average distance of vectors coming from the class  $\theta_q$  to the nearest reference vector representing the class other than  $\theta_q$ .

### 5.2. Post-Processing Results

Fig. 3 displays two examples of segmented and post-processed pulp images. The segmentation was obtained through pixel-wise classification based on a minimum distance to a reference pattern classifier. Image pixels assigned to the background class – *White* – are assumed to be transparent in the visualization adopted in Fig. 3 and, therefore, left unaltered if compared to the original images. Image pixels assigned to the classes *Cyan*, *Magenta*, *Yellow*, *Green*, and *Black* are highlighted and represented by colour corresponding to the class name. The speck detection results shown in Fig. 3 can be a point of contention, since some specks seem not to be detected. However, observe that the sensitivity of the speck detection system was adjusted so, that only the specks located on the top of the test sample are detected. Due to the light scattering in the test sample, shadows of some specks located inside the test samples also appear in the images. The original image of the one shown on the right-hand side of Fig. 3 is the image presented on the right-hand side of Fig. 2. Thus, one can contrast the images and examine the speck detection results.

It is obvious that it is not an easy task to assess the classification results for such images. Only careful visual inspection can be applied. Such an inspection has shown that the post-processing technique developed improves classification accuracy of the colour images. The post-processing results depend, to some extent, on the size of the post-processing window. We varied the size of the window from  $3 \times 3$  to  $7 \times 7$  pixels. For the

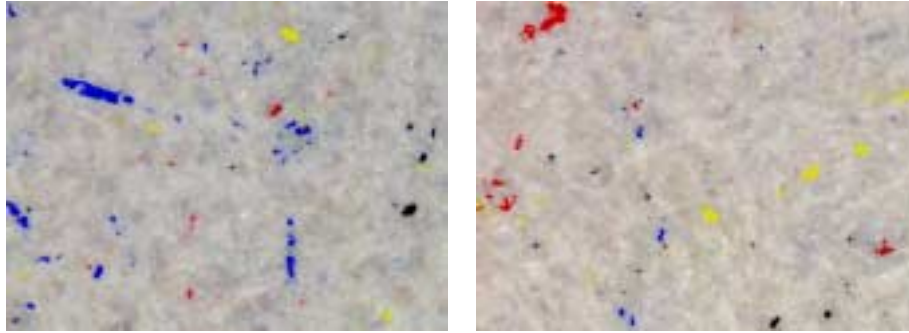


Fig. 3. Two examples of segmented and post-processed pulp images.

pulp images, the best results – as judged by the visual inspection – were obtained using the  $3 \times 3$  window.

Fig. 4 presents an image of an enlarged view of a multi-coloured speck before and after the post-processing. The size of the post-processing window was set to  $3 \times 3$  in this example. As it can be seen from Fig. 4, even a single pixel, entirely surrounded by neighbours from a different class, may retain its class label during the post-processing. Such a post-processing result occurs, if the neighbours of the pixel being considered are quite uncertain about the class label they possess, while high certainty was observed when assigning a label to the pixel being considered. Such an adaptivity is the characteristic feature of the post-processing technique developed.

Concerning the influence of the parameters  $\beta_0^{dist}$ ,  $\beta_0^{rival}$ ,  $\beta_{pq}$ , and  $\alpha_p$  on the post-processing results, it should be observed, that these parameters have trade-off relations between each other. The parameters  $\beta_0^{dist}$ ,  $\beta_0^{rival}$ , and  $\beta_{pq}$  affect the subdivision of our belief obtained from some classification result between the atomic hypotheses  $\theta_i$  and the frame of discernment  $\Theta$ . The fact of using values of these parameters less than unity indicates that, even in the case of “*perfect match*” there is some uncertainty that the pixel being analyzed  $\mathbf{x}^j$  belongs to the matching class  $\theta_q$ . By the perfect match we mean here a zero minimum distance  $d(\mathbf{x}^j, \mathbf{w}_q^k)$ .

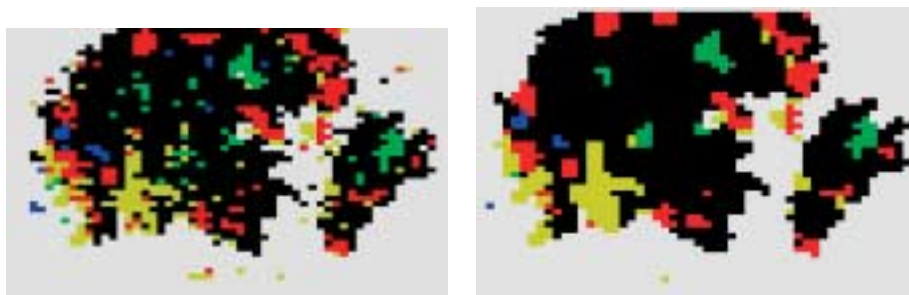


Fig. 4. **Left:** An example of a speck image before the post-processing. **Right:** The same image after the post-processing.

When using a 2 GHz PC and the post-processing window of  $3 \times 3$  pixels, the average processing time of about 1 second was observed for an image of  $768 \times 576$  pixels. Such a processing speed is acceptable for the application at hand.

## 6. Conclusions

We presented an approach based on the evidence theory to post-processing of pixel-wise classified images. Each neighbour of a pixel being analyzed is considered as an item of evidence supporting particular hypotheses regarding the class label of that pixel. Basic belief masses are obtained for each of the neighbours and aggregated according to the rule of orthogonal sum. The final label of the pixel is chosen according to the maximum of the belief function. The technique allows exploiting information from both the original image and the classified image, and takes into account uncertainty, with which labels to pixels of the classified image were assigned. The characteristic feature of the post-processing technique developed is its adaptivity. Even a single pixel, entirely surrounded by neighbours from a different class, may retain its class label during the post-processing.

## References

- Bloch, I. (1996). Some aspects of Dempster–Shafer evidence theory for classification of multi-modality medical images taking partial volume effect into account. *Pattern Recognition Letters*, **17**, 905–919.
- Bouchaffra, D., V. Govindaraju, S.N. Srihari (1999). Postprocessing of recognized strings using nonstationary Markovian models. *IEEE Trans Pattern Analysis Machine Intelligence*, **20**, 990–999.
- Chen, S.Y., W.C. Lin, C.T. Chen (1993). Evidential reasoning based on Dempster–Shafer theory and its application to medical image analysis. *SPIE*, **2032**, 35–46.
- Chen, M.Y., A. Kundu, J. Zhou (1994). Off-line handwritten word recognition using a hidden Markov model type stochastic network. *IEEE Trans Pattern Analysis Machine Intelligence*, **16**, 481–496.
- Chen, T.Q., Y. Lu (2002). Color image segmentation – an innovative approach. *Pattern Recognition*, **35**, 395–405.
- Cheng, H.D., X.H. Jiang, Y. Sun, J. Wang (2001). Color image segmentation: advances and prospects. *Pattern Recognition*, **34**, 2259–2281.
- Cheng, H.D., X.H. Jiang, J. Wang (2002). Color image segmentation based on hamogram thresholding and region merging. *Pattern Recognition*, **35**, 373–393.
- van Cleynenbreugel, J., S. Osinga, F. Fierens, P. Suetens, A. Oosterlinck (1991). Road extraction from multi-temporal satellite images by an evidential reasoning approach. *Pattern Recognition Letters*, **12**, 371–380.
- Denoeux, T. (1995). A  $k$ -nearest neighbor classification rule based on Dempster–Shafer theory. *IEEE Trans Systems, Man and Cybernetics – Part B*, **25**, 804–813.
- Gao, J., J. Zhang, M. Fleming (2002). Novel technique for multiresolution color image segmentation. *Optical Engineering*, **41**, 608–614.
- Greenspan, H., J. Goldberger, I. Eshet (2001). Mixture model for face-color modeling and segmentation. *Pattern Recognition Letters*, **22**, 1525–1536.
- Huang, H.Y., Y.S. Chen, W.H. Hsu (2002). Color image segmentation using a self-organizing map algorithm. *Journal of Electronic Imaging*, **11**, 136–168.
- Hunt, R.W.G. (1991). *Measuring Colour*. Ellis Horwood.
- Kurugollu, F., B. Sankur, A.E. Harmanci (2001). Color image segmentation using histogram multithresholding and fusion. *Image and Vision Computing*, **19**, 915–928.
- LeHegarat–Mascle, S., I. Bloch, D. Vidal–Madjar (1997). Application of Dempster–Shafer evidence theory to unsupervised classification in multisource remote sensing. *IEEE Trans Geoscience Remote Sensing*, **35**, 1018–1031.

- Li, C.H., P.C. Yuen (2000). Regularized color clustering in medical image database. *IEEE Trans Medical Imaging*, **19**, 1150–1155.
- Mirmehdi, M., M. Petrou (2000). Segmentation of color textures. *IEEE Trans Pattern Analysis Machine Intelligence*, **22**, 142–159.
- Papamarkos, N., C. Strouthopoulos, I. Andreadis (2000). Multithresholding of colour and gray-level images through a neural network technique. *Image and Vision Computing*, **18**, 213–222.
- Pinz, A., M. Prantl, H. Ganster, H. Kopp–Borotschnig (1996). Active fusion – A new method applied to remote sensing image interpretation. *Pattern Recognition Letters*, **17**, 1349–1359.
- Onyango, C.M., J.A. Marchant (2001). Physics-based colour image segmentation for scenes containing vegetation and soil. *Image and Vision Computing*, **19**, 523–538.
- Shafer, G. (1976). *A Mathematical Theory of Evidence*. Princeton University Press, Princeton, NJ.
- Y.Song, K., M. Petrou, J. Kittler (1995). Texture crack detection. *Machine Vision and Applications*, **8**, 63–76.
- Tominaga, S. (1992). Color classification of natural color images. *Color Research and Application*, **17**, 230–239.
- Trahanias, P.E., A.N. Venetsanopoulos (1996). Vector order statistics operators as color edge detectors. *IEEE Trans Systems, Man, & Cybernetics – Part B: Cybernetics*, **26**, 135–163.
- Tremeau, A., N. Borel (1997). A region growing and merging algorithm to color segmentation. *Pattern Recognition*, **30**, 1191–1203.
- Verikas, A., K. Malmqvist (1995). Increasing colour image segmentation accuracy by means of fuzzy post-processing. In *Proceedings of the IEEE International Conference on Artificial Neural Networks, ICANN-95*, Vol. 4. Perth, Australia. pp. 1713–1718.
- Verikas, A., K. Malmqvist, L. Bergman (1994). Including context analysis for discrimination between pictures of highly similar colors. In *Proceedings of the Symposium on Image Analysis*. Halmstad, Sweden. pp. 85–89.
- Verikas, A., K. Malmqvist, L. Bergman (2000). Neural networks based colour measuring for process monitoring and control in multicoloured newspaper printing. *Neural Computing & Applications*, **9**, 227–242.
- Verikas, A., K. Malmqvist, L. Bergman, K. Nilsson (1993). Color classification by neural network. In *Proceedings of the International Conference on Neural Networks and Their Industrial & Cognitive Applications*. Nimes, France. pp. 329–338.
- Verikas, A., K. Malmqvist, M. Bachauskene, L. Bergman, K. Nilsson (1994). Hierarchical neural network for color classification. In *Proceedings of the IEEE International Conference on Neural Networks*, Vol. 5. Orlando, Florida, USA. pp. 2938–2941.
- Verikas, A., K. Malmqvist, M. Bacauskiene, L. Bergman (2000). Monitoring the de-inking process through neural network-based colour image analysis. *Neural Computing & Applications*, **9**, 142–151.
- Verikas, A., M. Bacauskiene, K. Malmqvist (2003). Learning an adaptive dissimilarity measure for nearest neighbour classification. *Neural Computing & Applications*, **11**, 203–209.
- Wyszecki, G., W.S. Stiles (1982). *Color Science. Concepts and Methods, Quantitative Data and Formulae*. 2nd edn. John Wiley & Sons.
- Xu, L., A. Krzyzak, C.Y. Suen (1992). Methods for combining multiple classifiers and their applications to handwriting recognition. *IEEE Trans Systems, Man, and Cybernetics*, **22**, 418–435.
- Xu, L., M. Jackowski, A. Goshtasby, D. Roseman, S. Bines, C. Yu, A. Dhawan, A. Huntley (1999). Segmentation of skin cancer images. *Image and Vision Computing*, **17**, 65–74.

**M. Bacauskiene** is a senior researcher in the Department of Applied Electronics at Kaunas University of Technology, Lithuania. Her research interests include neural networks, image processing, pattern recognition, and fuzzy logic. She participated in various research projects and published numerous papers in these areas.

**A. Verikas** is currently holding a professor position at both Halmstad University, Sweden and Kaunas University of Technology, Lithuania. His research interests include image processing, pattern recognition, neural networks, fuzzy logic, and visual media technology. He is a member of the International Pattern Recognition Society, European Neural Network Society, International Association of Science and Technology for Development, and a member of the IEEE.

**Akivaizdumo teorija grįstas spalvotų vaizdų analize būdas**

Marija BACAUSKIENE, Antanas VERIKAS

Pateikiamas Dempster–Shafer akivaizdumo teorija grįstas būdas spalvoto klasifikuoto vaizdo kontekstinei analizei. Tariama, kad kiekvienas analizuojamo vaizdo pikselio kaimynas suteikia porciją informacijos palaikančios hipotezė apie pikselio priklausymą tam tikrai klasei. Palaikymo stiprumas apibrėžiamas kaip priklausymo klasei abejonės laipsnio bei atstumo tarp nagrinėjamo pikselio ir kaimyno funkcija. Pikselio kaimynai apibrėžiami kontekstinės analizės langu. Pikselio kaimynų suteikta informacija apjungiamą pagal ortogonalios sumos taisyklę ir naudojama galutiniam sprendimui apie pikselio priklausymą tam tikrai klasei priimti.